Supplement of Clim. Past, 14, 763–788, 2018
https://doi.org/10.5194/cp-14-763-2018-supplement

Supplement of

Novel automated inversion algorithm for temperature reconstruction using gas isotopes from ice cores

Michael Döring and Markus C. Leuenberger

Correspondence to: Michael Döring (doering@climate.unibe.ch)

S1: Accumulation-rate data:

Originally, the accumulation rates used to feed the ice-flow model were optimised in order to match the time scale from Meese et al. (1994) for the Holocene, based on annual-layer-counting. Seierstad et al. (2014) transferred the GISP2 chronology to the GICC05 reference timeframe using multiple match points to the NGRIP and GRIP ice cores, both already on GICC05. We used these match points and modified the GISP2 ages in between match points linearly in order to match exactly the GICC05 duration for the considered interval duration. This way, the detailed GISP2 annual-layer-counting information is kept, but is only stretched/compressed in time. This was done for all intervals in between two match points. The accumulation data were then re-calculated accordingly as obviously this is needed in order to keep the same total amount of ice accumulated at the GISP2 site.

S2: Sensitivity study on the impact of filtering of accumulation on the model outputs and the influence of the accumulation on Holocene $\delta^{15}N$ data

In order to investigate the influence of smoothing of the accumulation-rate data on the model outputs, the high resolution accumulation-rate dataset in the time window of 20 yr to 12000 yr (Fig. 2a) were low-pass filtered with cut-off-periods between 20 yr and 500 yr, and used to drive the firn model. The surface-temperature input was set as constant with a value of -31 °C for this time window. Then, the deviations of the filtered from the unfiltered accumulation rates and model outputs were calculated. Figure S2 shows the absolute (I) as well as the relative deviations (II) (relative to the unfiltered scenario) as a function of the cut-off-periods for the accumulation-rate input-data, $\delta^{15}N$, and LID model outputs. Regarding the standard deviation (1σ) of the relative accumulation deviations as a measure for the mean deviation of the filtered minus the unfiltered values show that filtering the accumulation rates leads to a mean deviation of about 20 % between the filtered and unfiltered accumulation-rate data, depending on the used cut-off-period (see Fig. S2IIa). We use the mean 99 % quantile of the same analysis (Fig. S2IIb) as a measure for the maximum deviation between the filtered and unfiltered values. The filtering clearly leads to a maximum accumulation-rate deviation of about 50 %. The comparison of the related deviations in $\delta^{15}N$ and LID outputs reveals that the changes in the accumulation rates do not lead to a change in the same order for the model outputs. Indeed, the filtering of the accumulation-rate data lead to deviations of less than 0.6 % and less than 1.5 % for the mean and the maximum $\delta^{15}N$ and LID deviations, respectively (Fig. S2IIc,d). Therefore, it can be argued that a low-pass filtering of the accumulation rates for cut-off-periods between 20 yr and 500 yr does only have a small impact on the model outputs as long as the major trends are being conserved, because the filtering does not modify the mean accumulation. This result is expected due to the fact that the LID and finally $\delta^{15}N$ changes are the result of the integration of the accumulation over the whole firn column. The integration-time corresponds to the age of the ice at the LID, which is in the order of 200 yr for the Holocene in Greenland.

Finally, we test which fraction of the measured $\delta^{15}N$ variations can be attributed to accumulation changes. For this, we perform a sensitivity experiment (Fig. S3) where the temperature input was set as a constant value of -31 °C, and used together with the high-resolution accumulation-rate data (Fig. 2a) to model the LID (Fig. S3a) and $\delta^{15}N$ (Fig. S3b) values. Due to the absence of temperature changes, only the accumulation-rate changes drive the evolution of the diffusive-column-height (LID) over time which modulates the $\delta^{15}N$ values. Next, the modelled $\delta^{15}N$ variations are compared to the $\delta^{15}N$ measurement data (Fig. 5III) (Kobashi et al., 2008b) to examine the influence of the accumulation-rate changes on changes in $\delta^{15}N$ for two cases. First, for the 8.2k event, the signal amplitude in $\delta^{15}N$ is about three times higher for the measured data compared to the modelled ones (measured data: $\Delta\delta^{15}N_{8.2k,meas} \approx 60$ permeg (one permeg equals 10^{-6}); modelled data: $\Delta\delta^{15}N_{8.2k,mod} \approx 20$ permeg). The comparison of the standard deviations of the measured data with the modelled $\delta^{15}N$ data for the last 10 kyr (both quantities were normalized with their respective means), shows an even higher deviation of the measured versus the modelled variabilities by a factor of about eight.

measured data: $\mathrm{std}[\delta^{15}N_{10kyr,meas} - \mathrm{mean}(\delta^{15}N_{10kyr,meas})] \approx 37$ permeg;

modelled data: $\mathrm{std}[\delta^{15}N_{10kyr,mod} - \mathrm{mean}(\delta^{15}N_{10kyr,mod})] \approx 4.5$ permeg;

This analysis supports our assumption that the accumulation-rate history alone cannot fully explain the observed variability in $\delta^{15}N$ during the Holocene, and gives an upper limit for the contribution of the accumulation rate to the $\delta^{15}N$ signal. Therefore, the remaining part of the measured $\delta^{15}N$ variations has to be related to changes in surface temperature.

S3: Cross-correlation experiments

Several analyses were conducted in order to investigate the remaining mismatches in $\delta^{15}N$ and temperature after the high-frequency (step 3) and the correction part (step 4) of the reconstruction, respectively. First, the total misfit of $\delta^{15}N$ ($D_{\delta15Ntot}$) was separated into two fractions: gravitational ($D_{\delta15Ngrav}$) and thermal-diffusion mismatches ($D_{\delta15Ntherm}$) of $\delta^{15}N$ (Fig. S4). Figure S4 indicates that the main fraction of the total mismatch of $\delta^{15}N$ is due to the misfit of the thermal-diffusion component of the $\delta^{15}N$ signal, whereas the gravitational misfit of $\delta^{15}N$ has only a minor contribution. The ratio of the standard deviations $\sigma(D_{\delta15Ntherm})/\sigma(D_{\delta15Ngrav})$ is about 2.4 for the high-frequency solution, and about 2.3 for the corrected signal, showing that the misfit in the thermal-diffusion part is more than twice as high as in the gravitational component.

In Fig. S5a the xcf between the mismatch of total $\delta^{15}N$ ($D_{\delta15Ntot,hf}$) and the misfit of temperature ($D_{T,hf}$) is shown. The cross correlation leads to two extrema (r_{1a}=0.70, r_{2a}=-0.55) on two certain lags (l_{1a}=-2 yr, l_{2a}=+126 yr). In subplot (b) and (c) the same analysis is conducted between the mismatch of the gravitational ($D_{\delta15Ngrav,hf}$) component (b), and the thermal-diffusion ($D_{\delta15Ntherm,hf}$) component (c) of $\delta^{15}N$ and the temperature mismatch. It is obvious that the xcf of (a) is a combination of (b) and (c). The direct correlation on l_{1a} of (a) can be attributed mainly to the mismatch of the thermal-diffusion component of $\delta^{15}N$, whereas the negative correlation on l_{2a} is due to the mismatch of the gravitational component of $\delta^{15}N$. Regarding the xcfs of (a)-(c) at a certain lag l, i.e. l = 0 yr shows that here (and on most of the other lags) the correlations between $D_{\delta15Ngrav,hf}$ with $D_{T,hf}$ and $D_{\delta15Ntherm,hf}$ with $D_{T,hf}$ work in opposite directions, which makes it difficult to find a way to correct the remaining temperature mismatch using only information from $D_{\delta15Ntot,hf}$ for measurement data (when only $D_{\delta15Ntot,hf}$ is available). The correlation on l_{1a} in (a) is weakened, whereas the lag l_{2a} is shifted to higher values because of the superposition of gravitational and thermal-diffusion mismatch. Figure S5d shows also that the gravitational and thermal-diffusion mismatches of $\delta^{15}N$ are not independent, but the correlations at the extrema are relatively weak (r_{1d}=0.38, r_{2d}=-0.56). The negative correlation r_{2d} is a sign for the compensation effect between the gravitational and thermal-diffusion signals in $\delta^{15}N$ due to the high-frequency part of the reconstruction, whereas no explanation could be found for the positive correlation r_{1d}. The symmetric behaviour of the lags for r_{1d} and r_{2d} (l_{1d} = -88 yr ≈ -l_{2d}=93 yr) suggest that r_{1d} could be an artefact of a periodic behaviour of $D_{\delta15Ngrav,hf}$ and $D_{\delta15Ntherm,hf}$. Figures S6a-d show the same analysis after the correction part of the reconstruction. It is evident that in all cases the extrema in the different xcfs break down due to the correction of the temperature signal, which is the consequence of the decreasing mismatches of temperature as well as of $\delta^{15}N$. The comparison of the subplots (a), (b) and (c) also shows that the remaining temperature misfits after the correction are mainly driven by the mismatches of the thermal-diffusion signal of $\delta^{15}N$ with a minor contribution of the gravitational misfit.

Figures S5e-h show the cross-correlations between IF(t) used for the correction of the high-frequency temperature solution, and the temperature misfit (e), the mismatch of total $\delta^{15}N$ (f), the mismatch of the gravitational (g) and thermal-diffusion (h) component of the $\delta^{15}N$ signal calculated from the high-frequency temperature solution. For the correction, the cross-correlations (e) and (f) were used (see Sect. 2.1, step 4 and Fig. 3). Since for measured data neither information about the temperature mismatch (the true temperature is not known) nor about the mismatch of the components of $\delta^{15}N$ (gravitational, thermal-diffusion) are available, it is imperative that the symmetric behaviour between the xcf(IF(t), $D_{T,hf}$(t)) and inverted xcf(IF(t), $D_{\delta15Ntot,hf}$(t)) holds true. This criterion is fulfilled for all eight synthetic data scenarios and especially for H1-H3. The comparison of the subplots (f), (g) and (h) of Fig. S5 show the same findings as before, namely that the xcf for IF(t) versus $D_{\delta15Ntot,hf}$ is the combination of the xcfs of IF(t) versus $D_{\delta15Ngrav,hf}$ and IF(t) versus $D_{\delta15Ntherm,hf}$, and that the major fraction of $D_{\delta15Ntot,hf}$ is contributed from $D_{\delta15Ntherm,hf}$. The advantage to use IF(t) for the correction is the symmetry between the two cross-correlations, which is created by two factors. The first one is the allocation of the window mid position to the entries of IF, which leads to the symmetric behaviour of the gravitational and thermal-diffusion misfits. Second, the shifting of the window in 1 yr steps creating IF(t) over the whole data set leads to an averaged information, but even more importantly, to constant dependency between the temperature and $\delta^{15}N$ mismatches. This can be used later on to fit measured data.

The calculation of IF(t) was conducted for different window lengths ranging from 50 yr to 750 yr (Fig. S7). Also, the correction was calculated by using only xcf_{max} or xcf_{min} of IF(t) versus $D_{\delta15N,hf}$ for correcting the temperature input. Figures S7a,b show the remaining mismatches of $\delta^{15}N$ ($D_{\delta15N,corr}$) (a), and temperature ($D_{T,corr}$) (b) after the correction as a function of the used window length for IF(t). The analysis shows that for all investigated window lengths the correction reduces the mismatches of $\delta^{15}N$ and temperature, whatever correction mode was used (calculated with xcf_{max}, xcf_{min}, or both quantities, see comparison with the blue line in (a) and (b)). Furthermore, the correction works best for window lengths in the range of 100 yr to 300 yr with an optimum at 200 yr for all cases. This indicates that the maximum mean duration effect of a $\delta^{15}N$ mismatch creating a temperature mismatch (and vice versa) is in the same range for the investigated scenarios and such small deviations (low permeg level). It is also visible that the correction using both extrema (xcf_{max} and xcf_{min}) leads to a better correction as the approach using only one quantity. This is somehow surprising because the two extrema are the result of the periodicity of IF(t), $D_{\delta15N,hf}$ and $D_{T,hf}$. An explanation for this result could be that a larger section of the temperature time-series is corrected when both extrema are used for the correction, due to shifts in both directions. The correction using xcf_{max} only leads to a better fit than the one with xcf_{min}, which can be attributed to the higher correlation between IF(t) and $D_{\delta15N,hf}$. Figures S7e,f show the evolution of the lags corresponding to the two extrema for the cross-correlations between IF(t), and the $\delta^{15}N$ and temperature mismatches, respectively. The linear dependency between the lags and the window length (the lags are nearly half of the window length) is the result of the construction of IF(t), which means the averaging due to the integration in the window of this certain length and the symmetric behaviour due to the allocation of the window mid position to the entries of IF(t).

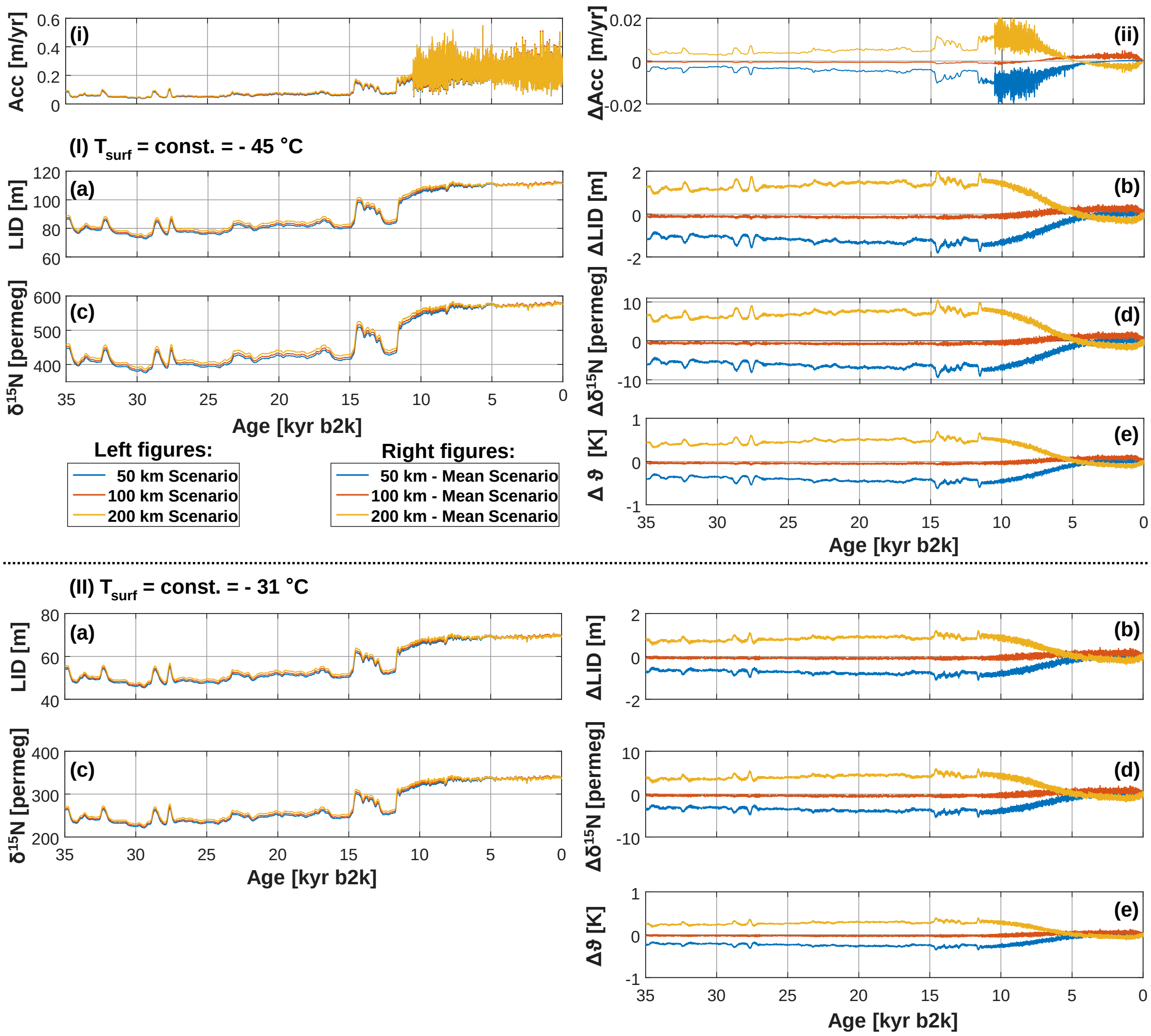

Figure S1: Possible accumulation-rate scenarios (i), the deviation from the averaged scenario (ii) and resulting modelled lock-in-depth (LID) (a) and $\delta^{15}N$ values (b) and deviations (c), (d), as well as, corresponding temperature uncertainties $\Delta\vartheta$ (e), for a constant temperature-input (I) -45 °C and (II) -31 °C.

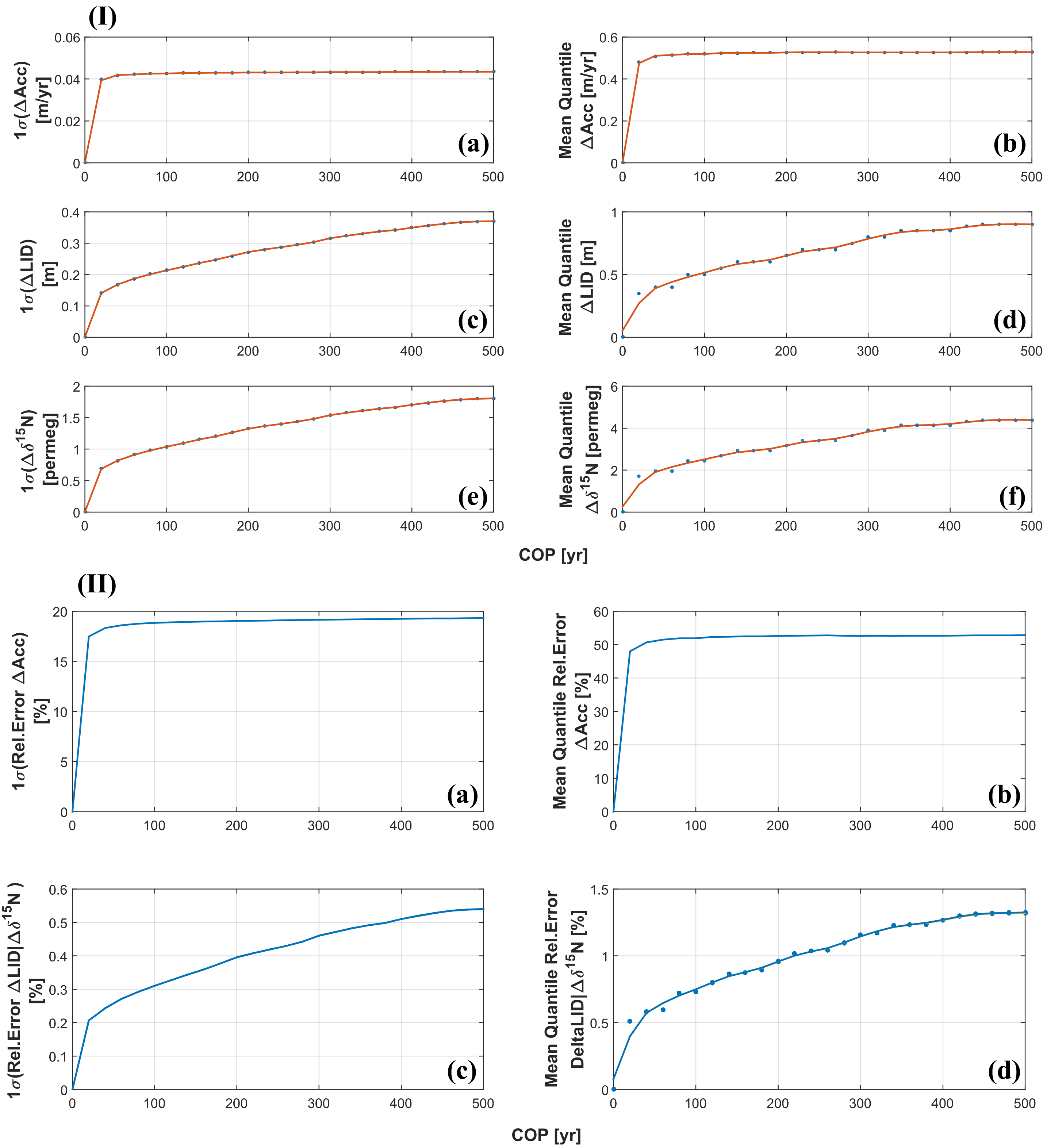

Figure S2: (I): Standard deviation (1σ) (a,c,e) and mean 99 % quantile (b,d,f) absolute deviations as a function of the cut-off-period (COP) for the last 10 kyr for: (a), (b) filtered minus unfiltered accumulation-rate data. (c), (d) modelled lock-in-depths (LID) using the filtered accumulation-rate scenarios minus LID time-series using the unfiltered accumulation-rate data. (e),(f) modelled $\delta^{15}N$ values using the filtered accumulation-rate scenarios minus $\delta^{15}N$ time-series using the unfiltered accumulation-rate data. (II): (a-d) Standard deviation (1σ) (a,c) and mean 99 % quantile (b,d) for the relative deviations compared to the unfiltered accumulation-rate scenario as a function of the cut-off-period for the last 10 kyr for: (a), (b) filtered minus unfiltered accumulation-rate data. (c), (d) LID and $\delta^{15}N$ deviations using the filtered accumulation-rate scenarios minus LID and $\delta^{15}N$ time-series using the unfiltered accumulation-rate data.

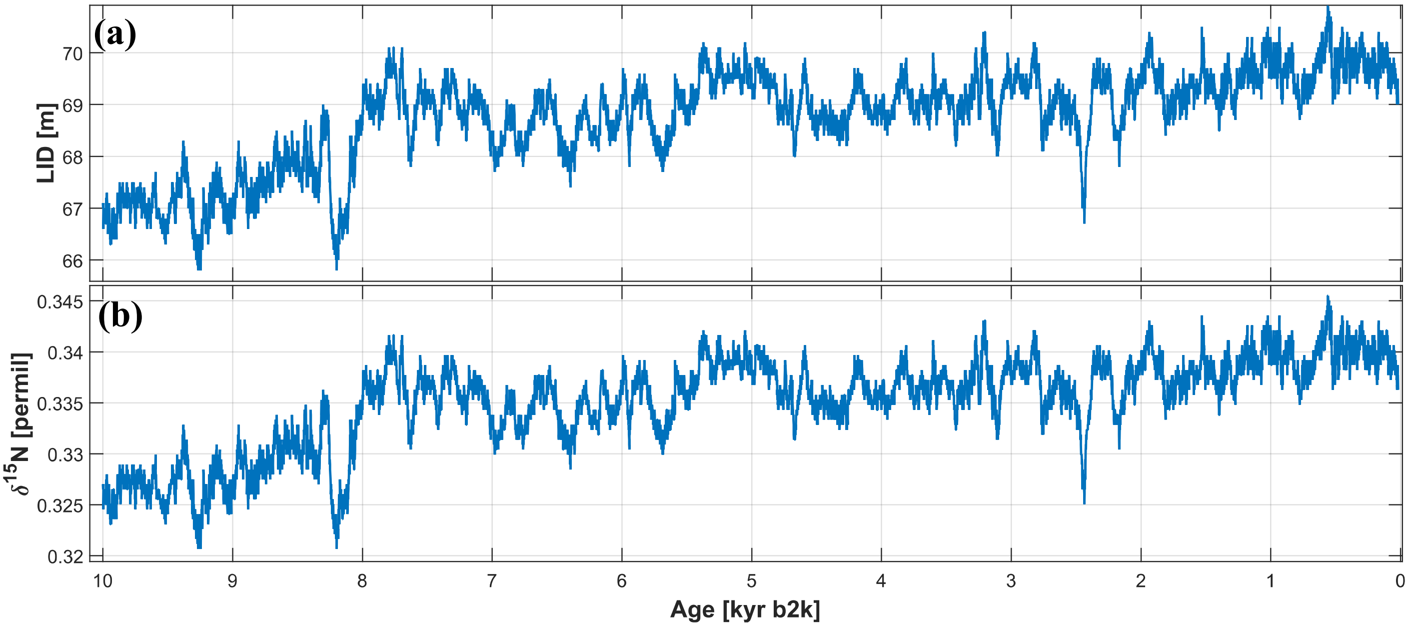

Figure S3: Lock-in-depth (LID) (a) and resulting $\delta^{15}N$ time-series (b) for the last 10 kyr using a constant surface-temperature input of -31 °C and the high resolution accumulation-rate input (Fig. 02a).

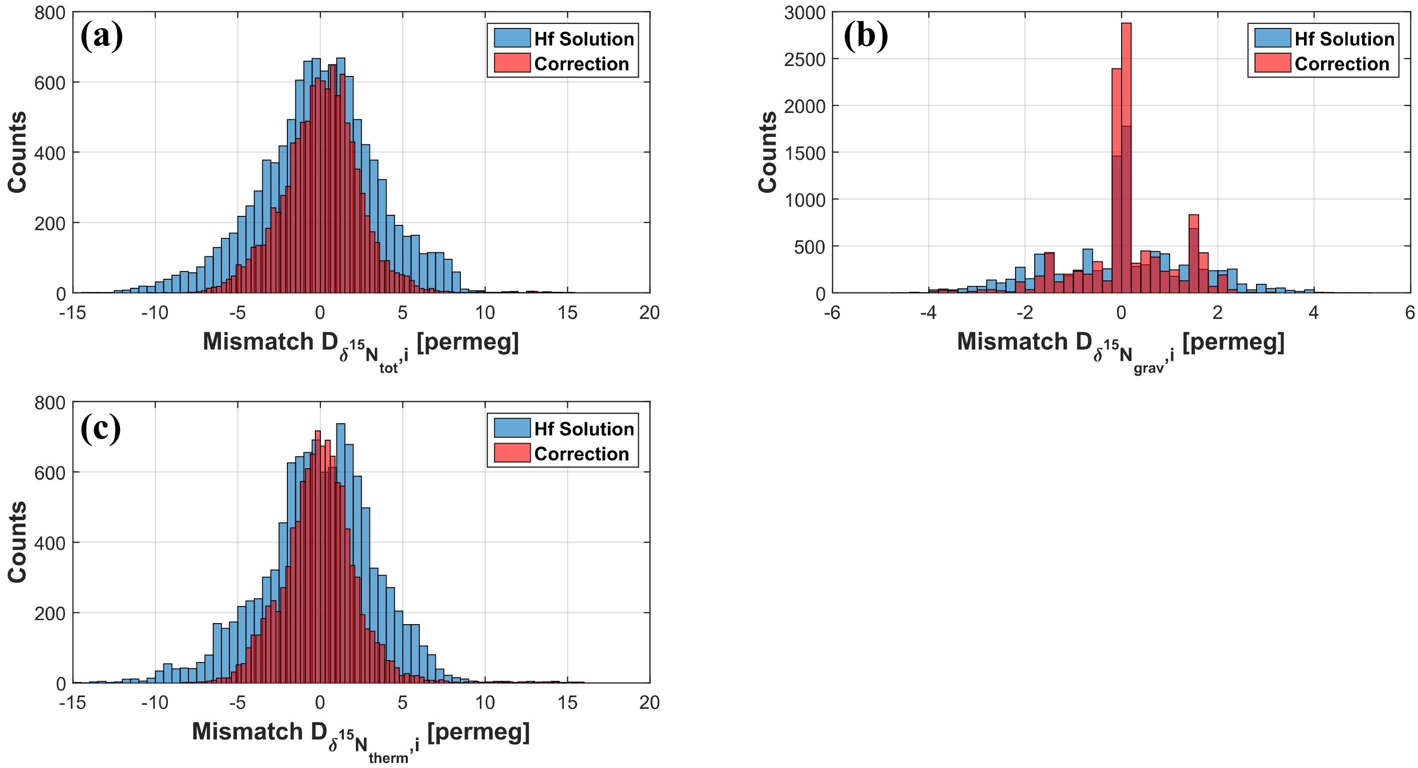

Figure S4: Histograms shows the pointwise mismatches $D_{\delta 15N,i}$ in $\delta^{15}N$ between the synthetic target data and the $\delta^{15}N$ solution of the high-frequency part (blue) and the correction part (red) for (a) the mismatch in total $\delta^{15}N$ ($D_{\delta 15Ntot,i}$), (b) in the gravitational ($D_{\delta 15Ngrav,i}$), and (c) in the thermal-diffusion component ($D_{\delta 15Ntherm,i}$) of $\delta^{15}N$ for the synthetic data scenario S1.

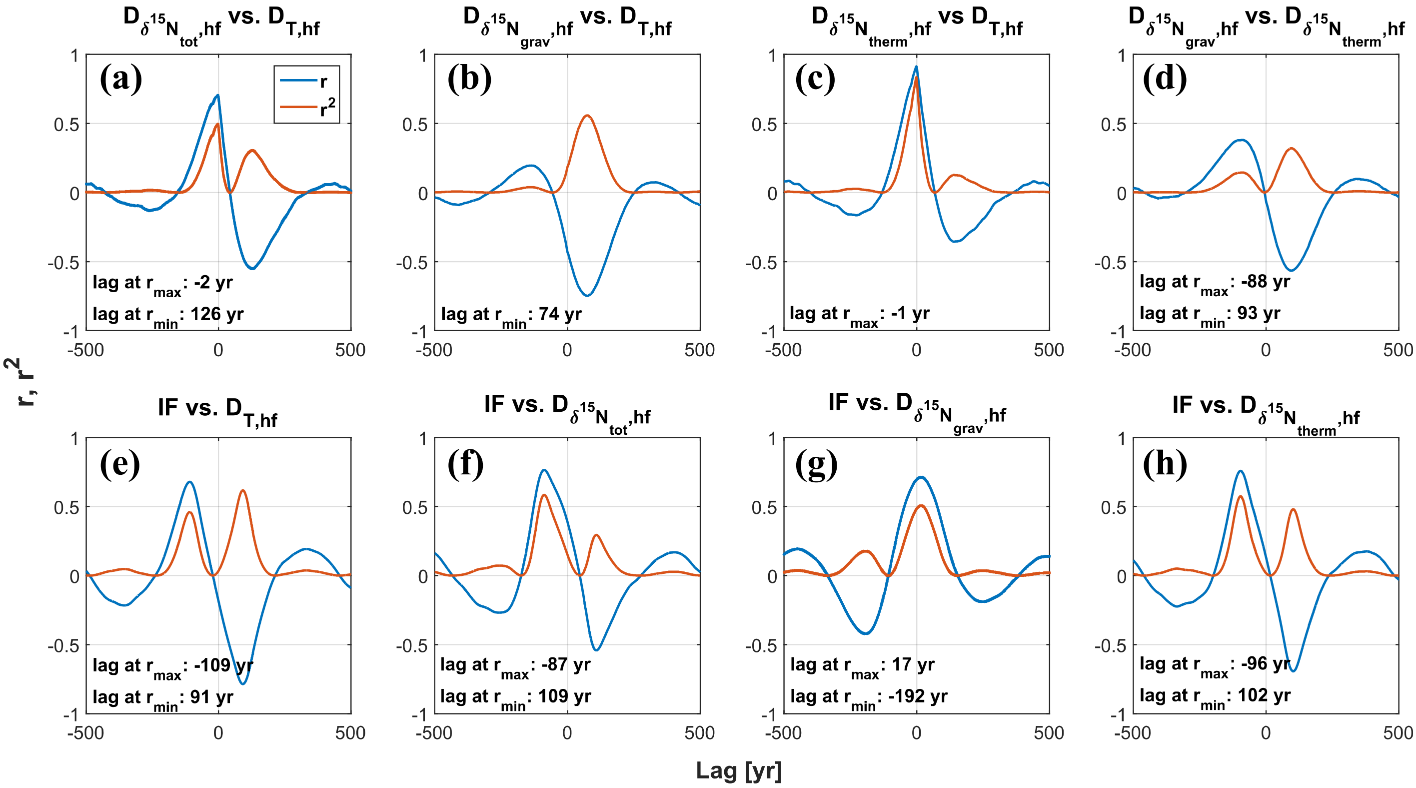

Figure S5: Cross-correlation-functions (xcf) for the scenario S1, investigating the dependencies between the temperature mismatch D_T, the mismatch $D_{\delta 15N}$ in total (tot), gravitational (grav) and thermo-diffusion (therm) fraction of the $\delta^{15}N$ signal and IF after the high-frequency part (hf); (a) xcf: $D_{\delta 15N,tot}$ vs. D_T; (b) xcf: $D_{\delta 15N,grav}$ vs. D_T; (c) xcf: $D_{\delta 15N,therm}$ vs. D_T; (d) xcf: $D_{\delta 15N,grav}$ vs. $D_{\delta 15N,therm}$; (e) xcf: IF vs. D_T; (f) xcf: IF vs. $D_{\delta 15N,tot}$; (g) xcf: IF vs. $D_{\delta 15N,grav}$ vs. D_T; (h) xcf: IF vs. $D_{\delta 15N,therm}$.

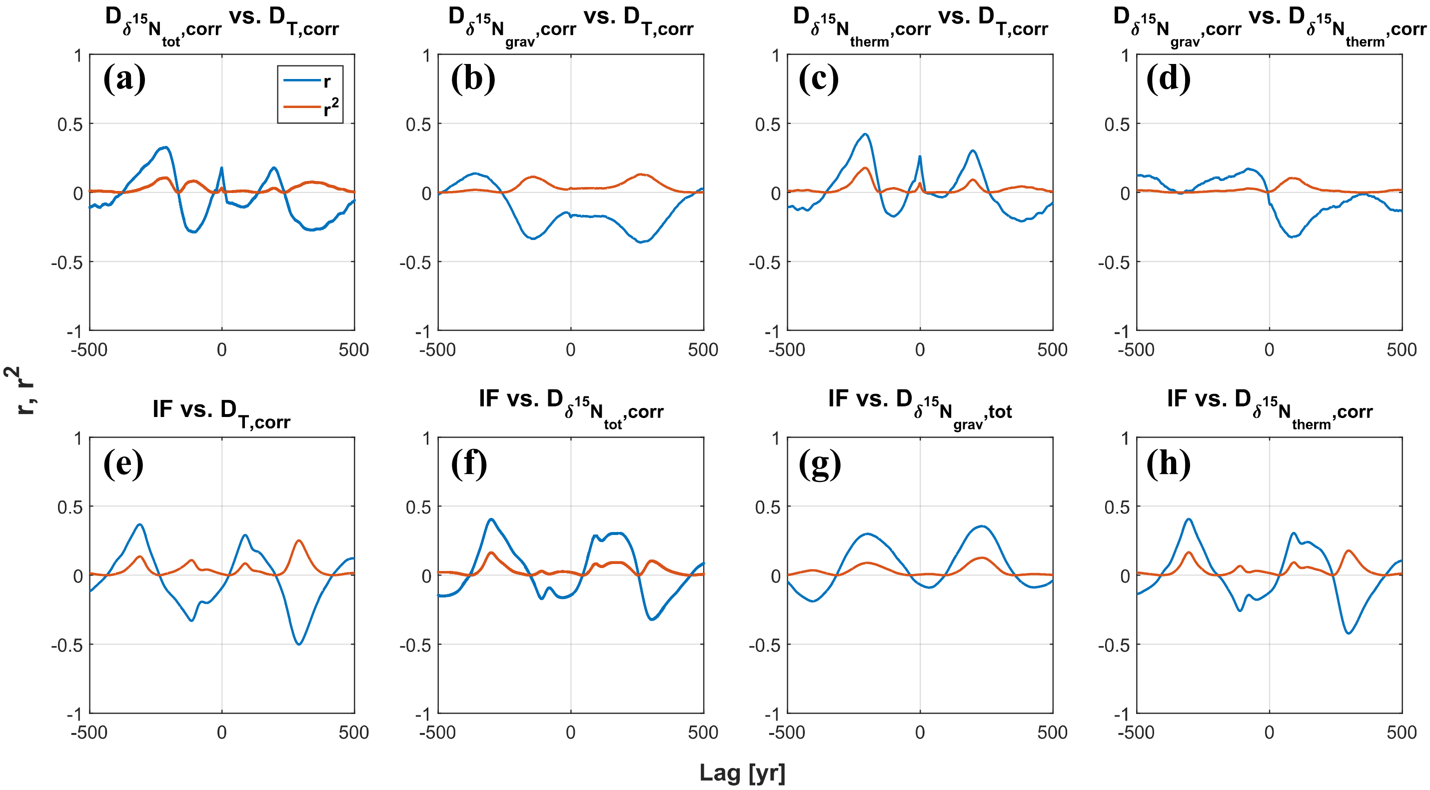

Figure S6: Cross-correlation-functions (xcf) for the scenario S1 investigating the dependencies between the temperature mismatch D_T, the mismatch $D_{\delta 15N}$ in total (tot), gravitational (grav) and thermo-diffusion fraction (therm) of the $\delta^{15}N$ signal and IF after the correction part (corr); (a) xcf: $D_{\delta 15N,tot}$ vs. D_T; (b) xcf: $D_{\delta 15N,grav}$ vs. D_T; (c) xcf: $D_{\delta 15N,therm}$ vs. D_T; (d) xcf: $D_{\delta 15N,grav}$ vs. $D_{\delta 15N,therm}$; (e) xcf: IF vs. D_T; (f) xcf: IF vs. $D_{\delta 15N,tot}$; (g) xcf: IF vs. $D_{\delta 15N,grav}$ vs. D_T; (h) xcf: IF vs. $D_{\delta 15N,therm}$.

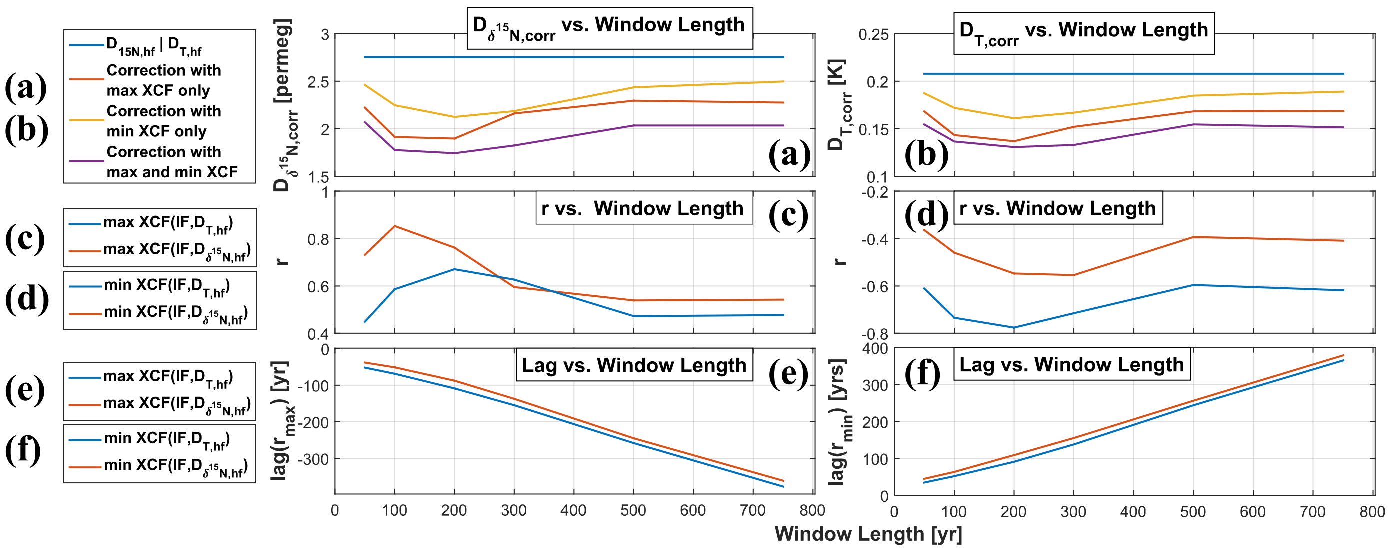

Figure S7: Dependency of the correction on the used window length (50 yr to 750 yr) for calculating IF for the scenario S1: (a) Remaining mismatch in $\delta^{15}N$ ($D_{\delta15N,corr}$) versus used window length for IF, after the correction of the temperature misfit $D_{T,hf}$ (blue line) and recalculation of $\delta^{15}N$, with the corrected temperature, using the maximum (red line) of xcf between IF and the $D_{\delta15N}$, the minimum (yellow line) of xcf and both (purple line), for the correction. (b) Remaining mismatch in temperature ($D_{T,corr}$) versus used window length for IF, after the correction of the temperature misfit $D_{T,hf}$ (blue line), using the maximum (red line) of xcf between IF and $D_{\delta15N}$, the minimum (yellow line) of xcf and both (purple line), for the correction. (c) Maximum (max xcf) correlation coefficient for the xcf between IF and D_T (blue line), and IF and $D_{\delta15N}$ (red line) as function of the used window length for IF. (d) Minimum (min xcf) correlation coefficient for the xcf between IF and D_T (blue line), and IF and $D_{\delta15N}$ (red line) as a function of the used window length for IF. (e) Related lag to the maximum (max xcf) correlation coefficient for the xcf between IF and D_T (blue line), and IF and $D_{\delta15N}$ (red line) as a function of the used window length for IF. (f) Related lag to the minimum (min xcf) correlation coefficient for the xcf between IF and D_T (blue line), and IF and $D_{\delta15N}$ (red line) as a function of the used window length for IF.